Chapter 4
Optical Transmission Spectrum: Analytical Technique, Results and Analysis

4.1 Introduction

In this work, one of the main objectives is study the effect of the argon dilution on the a-Si:H thin film produced by d.c plasma glow discharge of silane. UV-VIS-NIR optical transmission technique is used to investigate optical properties of the deposited thin film. Silane of flow-rates 5 and 20 sccm are diluted with argon of flow-rates 5, 10 and 15sccm during the deposition process to produce a-Si:H film. The other preparation parameters such as voltage, temperature and ionization currents are fixed during deposition. The deposition parameters of the a-Si:H film studied are detailed in Table 4.1.

Sample	flow-rate(sccm)		Pressure (±0.01mbar)		Argon/silane	Deposition
	Argon	Silane	Argon	Total	Flow-rate ratio	Time (±1min)
A1	0	20	0.00	0.46	0	60
A2	5	20	0.18	0.50	0.25	60
A3	10	20	0.26	0.50	0.5	120
A4	15	20	0.37	0.60	0.75	120
A5	0	5	0.00	0.10	0	60
A6	5	5	0.19	0.26	1	60
A7	10	5	0.30	0.37	2	60
A8	15	5	0.40	0.46	3	60

Table 4.1 : The deposition parameters of a-Si:H thin film samples studied in this work.

This chapter will begin with the discussion on the transmission spectra of the a-Si:H films produced and studied in this work. The calculation techniques used to determine the various optical parameters of the samples derived from the transmission spectra data are detailed in the following section. Results obtained from the calculations are then presented in section 4.4. The effects of argon dilution on the optical properties of the deposited samples are discussed in the following section. Finally, the optical results are analyzed at the end of this chapter.

4.2 Optical Transmission Spectra of a-Si:H Films.

The optical transmission spectra of the a-Si:H thin film samples studied in this work are scanned within the wavelength range of 250nm to 2500nm using the Jasco V-570 UV-VIS-NIR spectrophotometer. A total of eight a-Si:H films samples are scanned. Sample A1 is prepared from the d.c plasma glow discharge of pure silane at flow-rate of 20sccm while samples A2, A3 and A4 are prepared from the discharge of silane at the same flow-rate diluted with argon at flow-rates of 5, 10 and 15sccm respectively. Similarly, sample A5 is prepared from undiluted silane at flow-rate of 5sccm and samples A6, A7 and A8 are prepared from silane diluted in argon at flow-rates of 5, 10 and 15sccm respectively. The details of the preparation condition are presented in Table 4.1. The spectrum provides various informations on the optical properties and also the film thickness. Several technique and formula have been developed by scientists to determine the optical properties and film thickness accurately.

Figures 4.1 and Figures 4.2 present the spectra for the films prepared from silane flowing at 20sccm and 5sccm respectively diluted and undiluted in argon. Typical example of an optical transmission spectrum for a-Si:H film is illustrated by the spectrum

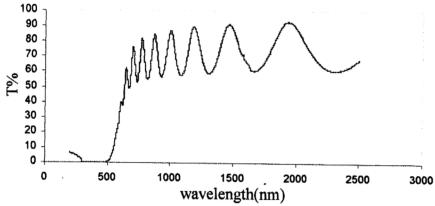

Figure 4.1(a)

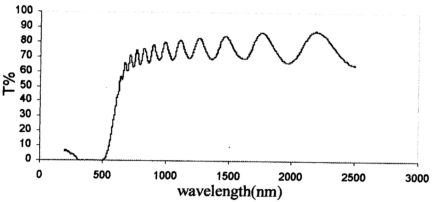

Figure 4.1(b)

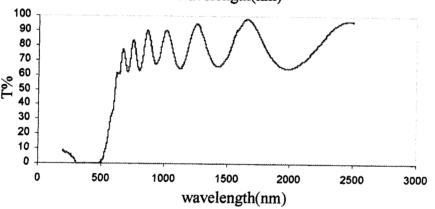

Figure 4.1(c)

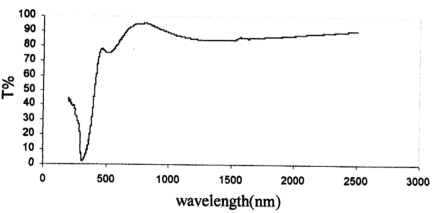

Figure 4.1(d)

Figure 4.1 : Optical transmission spectra of a-Si:H thin films deposited from the discharge of : (a) pure silane at flow-rates of 20sccm.
(b) 20sccm silane diluted in 5sccm argon.
(c) 20sccm silane diluted in 10sccm argon.
(d) 20sccm silane diluted in 15sccm argon.

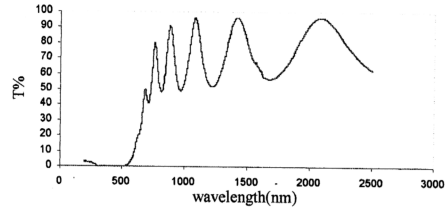

Figure 4.2(a)

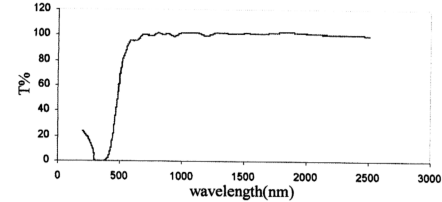

Figure 4.2(b)

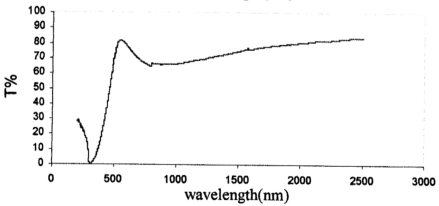

Figure 4.2(c)

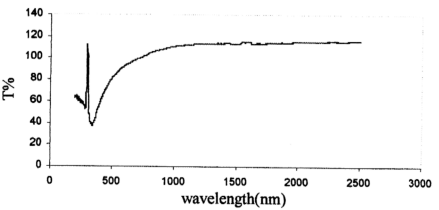

Figure 4.2(d)

Figure 4.2 : Optical transmission spectra of a-Si:H thin films deposited from the discharge of : (a) pure silane at flow-rates of 5sccm.
(b) 5sccm silane diluted in 5sccm argon.
(c) 5sccm silane diluted in 10sccm argon.
(d) 5sccm silane diluted in 15sccm argon.

produced by sample A1(Figure 4.1(a)). In the long wavelength region where the transmission percentage is high, sharp interference fringes are observed. A sharp decrease is observed in the region of 500nm wavelength. This region is referred to as the absorption edge where photon energy is totally absorbed by the film material. The pattern of the interference fringes is related to the refractive indices and the thickness of the film among the a-Si:H film samples. According to *E.A. Davis* [1], the magnitude of the intensity of the transmission spectrum and the presence of interference fringes can be used as a rough guide in comparing film thickness between samples. If the refractive indices of the samples are of the same magnitude, the thickness of the sample corresponds to the number of the interference fringes in the spectrum. The thicker films will have a larger number of interference fringes. By comparing the results of the transmission spectra in this work, one can observe that sample A1 has the largest number of the interference fringes when compared to the other samples. This indicates that sample A1 is the thickest when compared to the other samples however this is only a rough estimate since the refractive index do vary from sample to sample.

Besides thickness, the variation of refractive index with wavelength can also be deduced by roughly comparing the broadness of the interference fringes within the transmission spectrum. Within the same transmission spectrum, sharper interference fringe indicates higher refractive index as compared to a broad one. A typical example is the spectrum for sample A1 shown in Figure 4.1(a) which shows sharp interference fringes at shorter wavelength around 500nm and broadens at longer wavelength approaching 2500nm. This indicates that the refractive index is higher at the lower wavelength and decreases as the wavelength increases to 2500nm. This is expected since it is typical for refractive index to show dependence to wavelength in this manner. From the transmission spectra produced by all the samples, these typical trends are observed in all the spectra.

Figures 4.1(a) to 4.1(d) demonstrate the effect of argon dilution on the optical transmission spectra of the a-Si:H film prepared at low silane flow-rate of 5sccm. Diluting the silane with 5sccm, 10sccm and 15 sccm of argon produces high argon to silane flow-rate ratio of 1, 2 and 3. These samples are referred to as high argon dilution a-Si:H films in this work. Figures 4.2(a) to 4.2(d) on the other hand shows the optical transmission spectra of a-Si:H films prepared at high silane flow-rates of 20sccm. When diluted with argon at flow-rates of 5, 10 and 15sccm, the samples represent films with low argon to silane flow-rate ratios of 0.25, 0.5 and 0.75. These films are referred to as low argon dilution a-Si:H films in this work. In the low argon dilution films, increasing the argon to silane flow-rate ratio result in the broadening of the interference fringes. This effect indicates that the refractive index decreases with the higher argon dilution for these films. In the high argon dilution films, the interference fringes become very small and irregular for the samples with argon to silane flow-rate ratio of 1 where 5sccm of argon is diluted with 5sccm silane. For sample with argon to silane flow-rate ratio of 2, sharp fringes are observed and the interference fringes totally disappear when the argon to silane flow-rate ratio increases to 3. These samples show significant reduction in the refractive index, which could be due to the change in the film structure. Reduction in refractive index can indicate decrease in film density. In a-Si:H film, this effect can be due to the presence of microvoid structure or higher hydrogen content in the film.

Another important observation from the results of transmission spectra is the shift of the absorption edge as the argon/silane flow-rates ratio increases. The absorption edge is the wavelength representing of the minimum energy that needed for an electron in the film to transit from the valence band to conduction band during electron and photon interaction. This absorption edge time is indirectly related to the energy gap of the materials. The electronic transition starts at the absorption edge and the photon energy at

such wavelength will be absorbed by the film in direct way or indirectly through phonon transition. The optical transmission spectra for all the samples shown in figure 4.1 and figure 4.2 demonstrate that increasing the argon to silane flow-rates ratio shifts the absorption edge towards shorter wavelength. Thus, indirectly the energy gap broadens as the argon dilution increased. Since the shifting of absorption edge is towards shorter wavelength that in the region of ultraviolet, this shift is referred to as the blue shift.

The data of the transmission spectra of the samples is then used to determine the parameters of optical properties and film thickness of the samples using several calculation techniques. The details of these calculation techniques will be presented in the next section.

4.3 Analytical Technique.

The data of the optical transmission spectra are obtained using the Jasco V-570 spectrophotometer are imported into Microsoft Excel data files which are then used in determining the optical parameters such as optical energy gap, refractive index, Urbach Tail band width and film thickness. The calculation techniques will be briefly detailed in this part.

4.3.1 Determination of Thickness and Refractive Index

The thickness and refractive index of the film are determined using the techniques proposed by *J.C. Manifacier* [2] and *E.A. Davis* [3]. Combined T_{max} and T_{min} are considered as a continuous envelope function of λ in the transmission spectrum as illustrated in figure 4.3. From the transmission curve, the T_{max} and the T_{min} are obtained. The T_{max} and T_{min} values at long wavelength are used to determine the refractive index.

The refractive index of the sample is determined by using the following equation proposed by J.C. Manifacier.

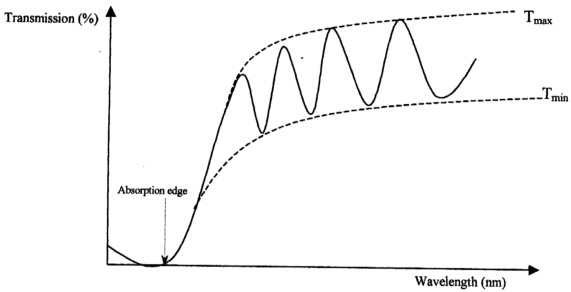

Figure 4.3 : The transmission spectrum which show the envelope method.

$$N = (n_o^2+n_1^2)/2+2n_on_1(T_{max}-T_{min})/(T_{max}T_{min}) \quad (4.1)$$

$$n = [N+(N^2-n_o^2n_1^2)^{1/2}]^{1/2} \quad (4.2)$$

The refractive index, n at the longest wavelength where the transmission percentage is close to 100% is determined using equations 4.1 and 4.2. These equations are most accurate when used in the highest transmission region [2]. The interference maxima and minima shown in figure 4.3 can be used to determine the optical thickness of the films, nd, where d is the geometrical thickness of the film. Successive extreme occur at wavelengths λ_m and λ_{m+1} given by equations

$$m\lambda_m = 2n\lambda_m t \quad (4.3)$$

$$(m+1)\,\lambda_{m+1} = 2n\lambda_{m+1}t \quad (4.4)$$

where m is the order of the fringe and takes integer value for a maximum and half integer value for a minimum. This technique was first proposed by *E.A. Davis* [4]. The orders of the fringes are determined by guessing a value of m and then a plot of nd versus λ is obtained. Incorrect value for m will produce an unphysical diverging behavior of nd as a function of increasing λ. Other sets of m values have to be tried until a dispersion curve of n with a trend that decreases very fast at short wavelength and saturates at long wavelength is obtained. The thickness is then determined at the longest wavelength where n was determined earlier using this n value and the order of the fringes at this λ, by using the equation 4.4. By using this thickness value, the n values at the wavelength of the maxima and minima of the interference fringes are determined. The n values are then fitted to the Cauchy Relation,

$$n = n_o + b/\lambda^2 \qquad (4.5)$$

In this equation, n_o is the static refractive index of the film obtained from the intercept of a plot of n versus $1/\lambda^2$ and b is obtained from the gradient of the plot. Using these values, the Cauchy Relation is used on the whole spectrum to obtain the dispersion curve of the refractive index with wavelength for the film. With exception of samples A7 and A8, this technique is used on all the samples to obtain the dispersion curve of n. The fitted n for except samples A7 and A8 that using other determination technique, which will be described later in this chapter.

4.3.2 Determination of Film Thickness and Refractive Index by Iteration Technique.

Since the transmission spectra of some samples (example samples A7 & A8) have one or no interference fringes at all, the technique presented in the previous section cannot be utilized to determine the film thickness, and refractive index, n. An iteration

technique propose by *K.M.M. Abo Hassan* in his Phd Thesis [5] uses the transmission, T and reflectance, R relation [6,7] at normal incidence below to determine n and d for these kind of films.

$$T = \frac{16n_1n_3n^2A}{C_1^2 + C_2^2A^2 + 2C_1C_2A\cos(4\pi nd/\lambda)} \quad (4.6)$$

$$R = \frac{B_1^2 + B_2^2A^2 + 2C_1C_2A\cos(4\pi nd/\lambda)}{C_1^2 + C_2^2A^2 + 2C_1C_2A\cos(4\pi nd/\lambda)} \quad (4.7)$$

Where $C_1 = (n+n_1)(n+n_3)$, $C_2 = (n-n_1)(n_3-n)$

$B^1 = (n-n_1)(n+n_3)$, $B_2 = (n+n_1)(n_3-n)$

$A = \exp(-4\pi kd/\lambda) = \exp(-\alpha d)$

and α is the absorption coefficient at the specification wavelength, λ. In this work, this technique is used with some modification. Equation 4.6 can be expressed in the form of

$$\left(C_2^2T\right)A^2 + \left(2C_1C_2T\cos\left\{\frac{4\pi nd}{\lambda}\right\} - 16n_1n_3n^2\right)A + C_1^2T = 0 \quad (4.8)$$

The roots of equation 4.8 are

$$A = \frac{-\left(2C_1C_2T\cos\left\{\frac{4\pi nd}{\lambda}\right\} - 16n_1n_3n^2\right) \pm \left(\left\{2C_1C_2T\cos\left[\frac{4\pi nd}{\lambda}\right] - 16n_1n_3n^2\right\}^2 - \left\{2C_1C_2T\right\}^2\right)^{1/2}}{2C_2^2T}$$

.....(4.9)

A rough estimate for the value of d is made by relating the calculated d value to the number of interference fringes. The d value chosen should be lower than the d value for the film with the lowest number of interference fringes. The n values are chosen from a range of values close to the n value of the bulk materials. Then, values chosen in this case are in the range of 1.6 to 2.5 . The value of d is used in equation 4.9 to calculated n for

each value of λ. An iteration command in LOTUS 1-2-3 software program is used to search for the correct n value using the following steps.

i. Each value of n as well as the values of the estimated film thickness, λ and the transmission fraction, T are substituted into equation 4.9 to calculate the two values of **A**. If the d value estimated is too far from the actual value, an infinite value for **A** is obtained. The d value is then reduced in steps of 20**A** until a finite **A** value is obtained. Then, the search for the correct value of A is done following the criteria : $0 < \mathbf{A} \leq 1$. The calculation continues for the whole range of n values. Many pair of solutions of n and A are obtained for each value of λ in the long wavelength region where T is almost 1 for in this region equation 4.6 and 4.7 are most accurate.

ii. These pair of solutions of n and A are used in equation 4.6 and 4.7 to calculated the calculated value for the transmission fraction, T_{cal} and reflectance, R_{cal}. The correct pair which are used in further calculations are the ones that give $T_{cal} \cong T_{exp}$ and $T_{cal} + R_{cal} = 1$ where T_{exp} is the experimental value for transmission fraction

iii. The calculation proceeded to the next value of λ until the whole of λ in the long wavelength region is covered. The n values are fitted to Cauchy Relation :

$$n = n_o + b/\lambda^2$$

Where n_o is the static refractive index and b is a constant to be determined from a plot of n versus $1/\lambda^2$. These n_o and b values are used on the whole spectrum to determine the n values at all wavelengths within the spectrum.

iv. The n values are then substituted into equation 4.6 to obtain the calculated value for T for the whole spectrum. Using the LOTUS 1-2-3, graphs of T_{cal} and T_{exp} are plotted versus wavelength for the whole spectrum. The n_o and b values are adjusted by increasing and decreasing the values in small steps, one at a time until the plots for T_{cal} and T_{exp} overlap. The n values from the adjusted n_o and b values are then used to

determine the absorption coefficient, α, optical energy gap, Eg and the Urbach Tail Bandwidth, E_e in the following section.

4.3.3 Determination of Absorption Coefficient.

When light of particular wavelength is incident on the a-Si:H film, it is transmitted, absorbed or reflected by the medium. Thus, it is dependent on the properties of the medium itself. Figure 4.4 shows that the transmission of light through a medium.

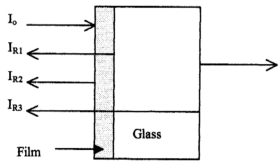

Figure 4.4 : The transmission of light through a medium.

Brodsky [8] provides the transmission of the two-layer film substrate.

$$T = \frac{(1-R_1)(1-R_2)(1-R_3)\exp(-\alpha d)}{(1-R_2R_3)\{1-[R_1R_2+R_1R_3(1-R_2)^2]\exp(-2\alpha d)\}} \qquad (4.10)$$

where R_1, R_2, R_3 are the reflectance at air-film, film substrate-air interface. D is the thickness of film.

The magnitude of the reflectivity must be known in order to determine adsorption coefficient,α. The reflectance R are given below:

$$R_1 = [(n-1)^2+k^2]/[(n+1)^2+k^2] \qquad (4.11a)$$

$$R_2 = [(n-n_1)^2+k^2]/[(n+n_1)^2+k^2] \qquad (4.11b)$$

$$R_3 = [(n-1)^2]/[(n+1)^2] \qquad (4.11c)$$

In these equations, n and n_1 are the corresponding indices of thin film and glass and k is the excitation coefficient for these materials. In this case, k = 0 since these materials are transparent. The equation (4.10) can be simplified as:

$$T = Ax/(1-B)(1-Cx^2) \tag{4.12}$$

where $A = (1-R_1)(1-R_2)(1-R_3)$ (4.13a)

$$B = R_2R_3 \tag{4.13b}$$

$$C = R_1R_2+R_1R_3(1-R_2)^2 \tag{4.13c}$$

$$X = \exp(-\alpha d) \tag{4.14}$$

$$(TC-TBC)x^2 + Ax - T(1-B) = 0 \tag{4.15}$$

The quadratic equation 4.15 produces solutions of

$$X = \frac{-A + \sqrt{A^2 - 4CT^2(1-B)^2}}{2CT(1-B)} \tag{4.16}$$

The absorption coefficient, α is expressed as

$$\alpha = (1/d)\ln(1/x) \tag{4.17}$$

where d is the thickness of the film.

4.3.4 Determination of Optical Energy Gap (E_g)

Optical energy gap is the small energy difference between the boundaries of the delocalized states in the valence band and the delocalized states in the conduction band. It is related to the absorption constant which proposed by *Tauc* [9] by the following equation

$$\alpha E = A(E - E_g)^2 \tag{4.18}$$

where E is the photon energy, E_g is the optical energy gap, α is the absorption coefficient and A is a constant for this equation.

The optical band gap (E_g) can be determined from the plot of $(\alpha E)^{1/2}$ as a function of E in the strong absorption region. The strong absorption region is as illustrated in figure 4.5. E_g is the minimum energy absorbed by the electron for transition from the valence band to the conduction band and is determined from the intercept of the most linear region at this plot on the energy axis. In this work, the energy (E) is calculated from the wavelength of the photon which, obtained from UV-VIS-NIR spectrophotometer and α is determine from the technique that described in section 4.3.3.

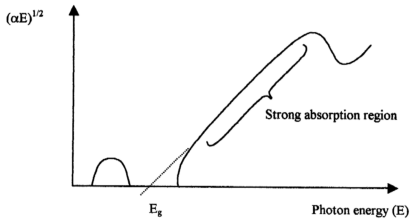

Figure 4.5 : Optical absorption edge of energy band gap E_g

4.3.5 Determination of Urbach Tail Bandwidth (E_e)

E_e represents of the extended width of the band tails and is related to the disorder in the thin film and usually referred to as the Urbach Tail bandwidth. This value is also derived from the optical transmission spectrum. The absorption coefficient has an exponential dependence close to the absorption edge. The absorption coefficient relation to the photon energy at this point can be expressed as :

$$\alpha = \alpha_o \exp[(E-E_1)/E_e] \qquad (4.19)$$

where, E is the photon energy, α_o and E_1 can be experimentally determined from a plot of $\ln\alpha$ versus E. The Urbarch Tail bandwidth, E_e is also obtained from this plot as equation 4.19 that can be expressed in the form

$$\ln\alpha = \frac{E}{E_e} + \left(\ln\alpha_o - \frac{E_1}{E_e}\right) \tag{4.20}$$

Samples	Argon/ SiH_4 Flow-rates Ratio	Thickness d (±25nm)	Deposition Rate (±0.06Å/s)	n (±0.05)	Optical energy (eV)	
					E_g ±0.01	E_e ±0.01
A1	0	1140	3.17	2.53	1.90	0.20
A2	0.25	1959	2.72	2.25	1.92	0.19
A3	0.5	1022	1.42	2.43	1.97	0.20
A4	0.75	757	2.10	2.0	2.68	0.11
A5	0	770	2.14	2.72	1.72	0.24
A6	1	1481	4.11	1.63	2.21	0.10
A7	2	1100	3.06	1.68	2.38	0.03
A8	3	950	2.64	1.72	1.88	0.07

Table 4.2 : The Results of thickness, deposition rates, n, E_g and E_e of a-Si:H films.

4.4 Effects of Argon Dilution on Deposition Rates of a-Si:H Films.

The effects of argon dilution on the various parameters obtained from the optical transmission spectrum will be analyzed. The samples analyzed will be categorized into two groups: (i) Low argon dilution and (ii) High argon dilution a-Si:H films. Samples A1 to A4 and samples A5 to A8 are categorized as low and high argon dilution a-Si:H films respectively. As tabulated in table 4.1, the low argon dilution films are prepared from the discharge of silane at flow-rates of 20sccm for sample A1 and silane at same flow-rates mixed with argon at flow-rates of 5sccm, 10sccm and 15sccm for samples A2, A3 and A4 respectively. Similarly, the high argon dilution films are prepared from the discharge of silane at flow-rate of 5sccm for sample A5 and silane at same flow-rates mixed with argon at flow-rates of 5sccm, 10sccm and 15sccm for samples A6, A7 and A8 respectively. These deposition parameters are tabulated in table 4.1.

The deposition rates of these samples are tabulated in table 4.2. Figure 4.6 illustrates the variation of the deposition rate with argon flow-rate for both the low and high argon dilution films. Without argon dilution, the deposition rate is higher for the higher silane flow-rate film. The film prepared at higher silane flow-rate of 20sccm is categorized in the low argon dilution films in this analysis. With argon dilution, the high argon dilution films are observed to have a higher growth rate comparatively. With argon flow-rate of 5sccm the low argon dilution film showed an increase in growth rate while the low argon dilution film showed a decrease in growth rate.

The increase in the growth rate can be attributed to argon incorporation into the film structure forming voids [11]. This result in a less compact structure thus increasing film thickness. The decrease in the growth rate on the other hand is due to bombardment of argon ions on the film surface producing an etching effect [12].

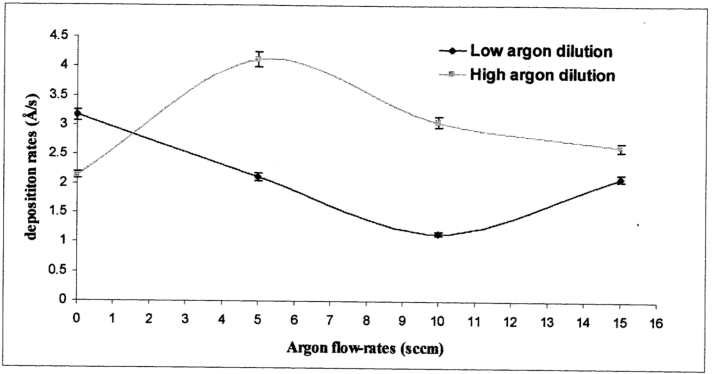

Figure 4.6 : Graph of deposition rates versus argon flow-rates for low argon dilution and high argon dilution.

Further increase in argon flow-rate to 10sccm results in argon ion bombardment in both films thus increasing the etching effect on the film structure. In the high argon dilution film, the etching effect continues but a lower rate is increased to 15sccm. The growth rate is increases in the low argon dilution film when the argon flow-rate is increased to 15sccm indicating the etching effect of argon ions bombardment have decreased and instead the argon ions get incorporated into the film structure resulting in void formation producing a less compact structure.

4.5 Effect of Argon Dilution on Refractive Index of a-Si:H Films

The refractive index of any material is usually related to the bulk density of the material. Higher refractive index materials usually demonstrate higher bulk density. Thus the compactness of a film structure can be deduced from the refractive index of the film and films with a more compact structure will have a higher refractive index.

Figure 4.7 shows the refractive index behaviors of both the high and low argon dilution a-Si:H films with argon flow-rate. Without argon dilution, the lower silane flow-rate a-Si:H film (5sccm) has a higher refractive index when compared to the higher silane flow-rate a-Si:H film (20sccm). This is expected since films deposited at lower flow-rates have a low growth rate and this results in a more uniform amorphous film structure. With argon dilution, high argon dilution films produce a more significant decrease in the refractive index. The refractive index generally is significantly lower for the high argon dilution films as the argon flow-rate is increase. Low bulk density is quoted to be due to columnar structure [13,14]. The above results suggests that high argon dilution in a-Si:H films produces more columnar structure in films.

Figure 4.7 : Graph of n versus argon flow-rates for low argon dilution and high argon dilution.

4.6 Effect of Argon Dilution on The Optical Energy Gap (E_g) in a-Si:H Films

The band gaps of pure amorphous silicon is about 1.3eV and hydrogenated amorphous silicon has a typical band gap between 1.7 to 2.0eV [15]. The variability in the energy gap value is strongly dependent on preparation conditions. Argon dilution of reactive silane during deposition of film is known to decrease the energy gap [13,16]. This effect is correlated to a decrease in oxygen contamination in the film.

Figure 4.8 shows the variation of the optical energy gap with argon flow-rate for high and low argon dilution films. Without argon dilution, the a-Si:H film prepared using the higher silane flow-rate of 20sccm has a higher optical energy gap. This film is categorized with the low argon dilution films. Higher silane flow-rates usually results in film with higher H concentration thus widen the energy gap. The optical energy gap of the low argon dilution films show insignificant dependence on argon flow-rate however it increase significantly to about 2.7eV when the argon flow-rate is increased to 15sccm. At this flow-rate, argon incorporated into the film must have affected the film microstructure. Referring to figure 4.7, at this flow-rate the refractive index of the film is also observed to decrease. The increase in the optical energy gap and decrease in the refractive index suggest that the film structure has become less compact thus reducing bulk density of the film.

In the high argon dilution films, increase in argon flow-rate results in the increase in the optical energy gap to a maximum at argon flow-rate of 10sccm and a significant decrease is observed when the argon flow-rate is increased to 15sccm. Argon ion incorporation is more significant when the argon to silane flow-rate ratio is larger than one as argon ion bombardment is more significant. The significant decrease observed when the argon flow-rate is 15sccm suggests that argon ion bombardment have a combined effect of argon ion incorporation into the film structure and also etching effect

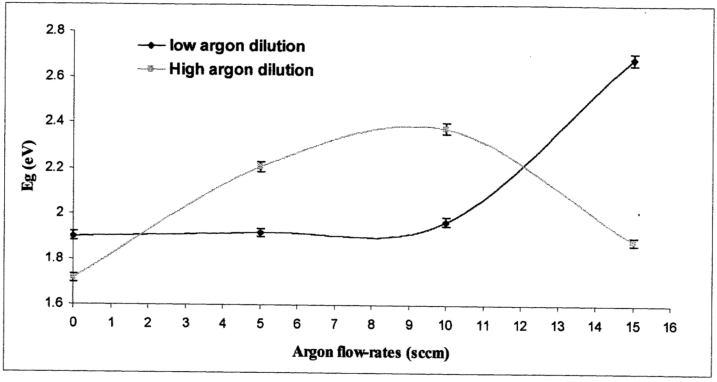

Figure 4.8 : Graph of Eg versus argon flow-rates for low argon dilution and high argon dilution.

of the film surface. These two effects when balanced could contributed to a homogeneous microstructural a-Si:H which is reflected from the decrease in the optical energy gap when the argon flow-rate is increased to 15sccm.

4.7 *Effect of Argon Dilution on The Urbach Tail Bandwidth (E_e) in a-Si:H Films.*

The Urbach Tail bandwidth, E_e is directly related to the magnitude of structure disorder in the a-Si:H. Structure disorders in this film are usually due to defects and dangling bonds concentration in the film structure. The variation of the Urbach Tail bandwidth with argon flow-rate for the high and low argon dilution films is shown in figure 4.9. Generally, the low argon dilution film exhibits higher E_e values compared to the high argon dilution films. Thus, the higher argon dilution films have a more ordered structure.

For the low argon dilution films, a significant decrease in E_e value is observed when the argon flow-rate is increased to 15sccm. As for the high argon dilution film, a significant decrease in the E_e value is observed when the argon flow-rate is as low as 5sccm and continue to decrease when the argon flow-rate is increased to 10sccm. A small but almost insignificant increase is observed when the argon flow-rate is increased to 15sccm. In both the low and high argon dilution films, significant increase in argon dilution has a pronounced effect on improving the film structure.

4.8 *Effects of Argon to Silane Flow-rate Ratio on The Optical Energy Gap, Refractive Index and Urbach Tail Bandwidth.*

In this section, the dependence of the optical energy gap (E_g), refractive index (n) and Urbach Tail bandwidth (E_e) on the argon to silane flow-rate ratio are studied. Figure 4.10 shows the variation of the E_g with argon to silane flow-rate ratio. An increase

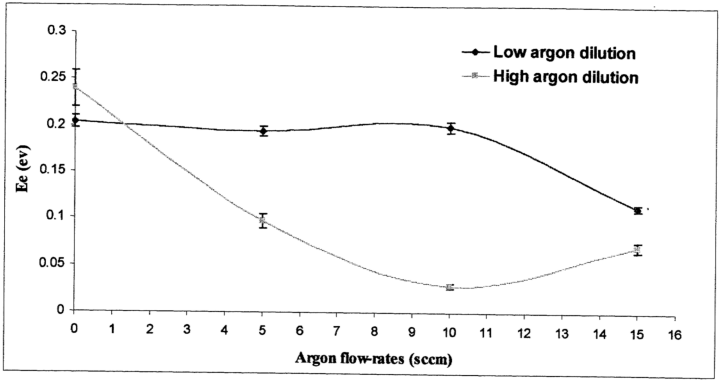

Figure 4.9 : The graph of Ee versus argon dilution flow-rates for low and high argon dilution.

in the E_g value is observed as the argon to silane flow-rate ratio is increase, reaches a maximum value when the flow-rate ratio is around 1.5 and decreased again with further increase in flow-rate ratio. The combined effect of argon incorporation into the film structure and the etching effect of the film structure contribute to the initial increase in the optical energy gap. The formation of homogeneous microstructural a-Si:H reduces defects and dangling bonds thus widens the optical energy gap. The latter decrease in the optical energy gap is due to increase in argon incorporation into the film structure and decrease the etching effect. A more disordered film structure reduces the optical energy gap.

Figure 4.11 demonstrates the dependence of n on the argon to silane flow-rate ratio. The refractive index of a film can be related to the bulk density of the film. Since the refractive index decrease with the increase in the argon to silane flow-rate ratio and saturates at high flow-rate ratio. The bulk density also behaves in a similar fashion. Thus, argon incorporation into the film structure can result in a less compact structure thus decreasing the film density.

Figure 4.12 shows a plot of Urbach Tail bandwidth, E_e versus argon to silane flow-rate ratio. The magnitude of E_e shows a decreasing trend initially with argon to silane flow-rate ratio and saturate at the lowest values as the argon to silane flow-rate ratio increases further. The result indicates that argon dilution increases the structural order in the film structure.

4.9 Conclusion

Argon is a metastable atom that never participates in the chemical reaction in the deposition of the amorphous silicon for at least up to the temperature of 400°C [17]. It acts only as a passive diluent gas but also plays an important role in the growth mechanism of amorphous silicon [18]. However, since argon is a heavy mass atom, the

effect of ion bombardment is significant accelerated at high speed by an electric field. From the results presented earlier in this chapter, argon dilution of silane in a-Si:H prepared by d.c plasma glow discharge has significant influence on the optical properties and structural order in the film structure.

Low argon dilution is observed to lower deposition rate however high argon dilution increases the deposition rate of a-Si:H film. The refractive index of the a-Si:H film decreases with high argon dilution indicating low bulk density. Low bulk density is associated to columnar structures in a-Si:H film. Thus, high argon dilution produces a-Si:H films with columnar structure. Since the trend of the Urbach Tail bandwidth, E_e and refractive index, n with argon to silane flow-rate ratio are similar, it can be deduced that the columnar structure in a-Si:H films produce a less compact structure. This effect can be further confirmed from the plot of E_e versus n, presented in figure 4.13, where E_e is directly proportional to n.

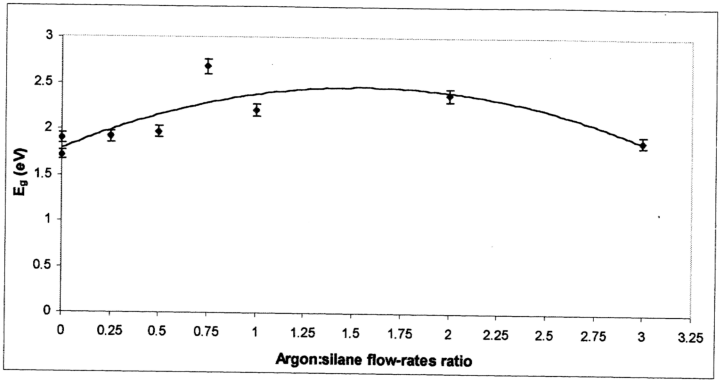

Figure 4.10 : Graph of E_g versus argon:silane flow-rates ratio for all the samples.

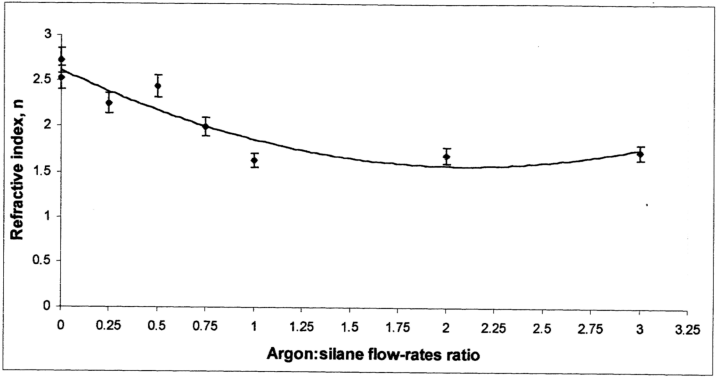

Figure 4.11 : Graph of refractive index (n) versus argon:silane flow-rates ratio for all the samples.

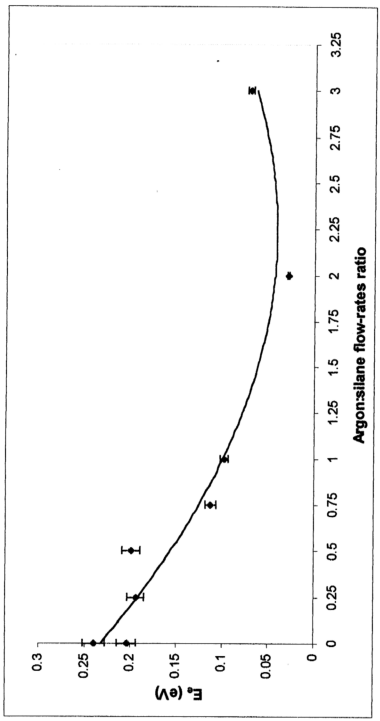

Figure 4.12 : Graph of E_0 versus argon:silane flow-rates ratio for all the samples.

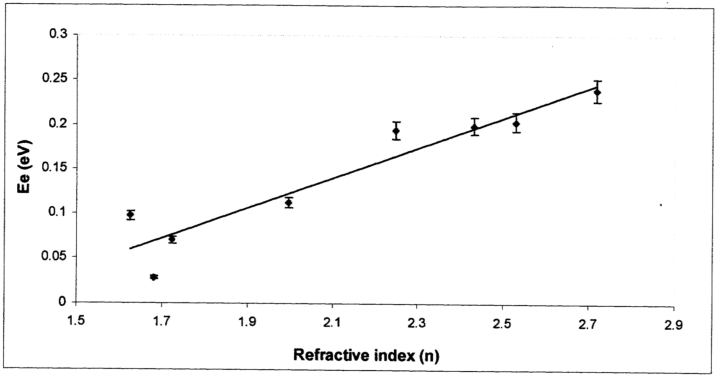

Figure 4.13 : Graph of E_e versus refractive index (n) for all a-Si:H films.

References

1) E.A. Davis, N.F. Mott, *Philos. Mag.* 22, 903 (1970).

2) J.C. Manifacier, J. Gasiot and J.P. Fillard, *J. Phys. E9*, 1002 (1976).

3) E.A. Davis, N. Piggins and S.C. Bayliss , *J. Phys. C20*, 4415 (1978).

4) E.A. Davis, N. Riggins, S.C. Bayliss , *J. Phys. C. Sol. Stat. Phys. E, 9*, 1002 (1978).

5) K.M.M. Abo Hassan, *PhD Thesis* , Universiti Malaya (1995)

6) J.C. Manifacier, J. Gasiot and J.P. Filland, *Journal of Physics E*, 9, 1002-1004 (1976).

7) S.P. Lyashenko and V.K. Miloslauskii, *Out. Spectroscopy B*, 80-81 (1964).

8) M.H. Brodsky, "*Amorphous Semiconductor*", Topic in Applied Physics, Vol. 36, Springer-Verlag (1979).

9) J. Tauc : *'Amorphous and Liquid Semiconductors'* , plenum press (1974).

10) M.H. Brodsky , *Energy Gap of amorphous silicon handbook*, wiley (1979).

11) T. Kanata, S.Yamasaki, K. Nakagawa, A. Matsuda, M.M and S.I , *J. of Non-Cryst. Solids 35 & 36*, 475-480, (1980).

12) R.A. Street, J.C. Knights and D.K. Biegelsen, *Phys. Rev. B*, 18, P.1880, (1978).

13) R.C. Ross, R. Messier, *J. Appl. Phys. (USA) Vol.56 No.2*, 347 (1984).

14) R.C. Ross, R. Messier, *J. Appl. Phys. (USA) Vol.52 No.8*, 5329 (1981).

15) E.C. Freeman, W. Paul, *EMIS Handbook Type Record RN=4219,"Energy Gap of Amorphous Silicon Films Prepared by Various Methods"*, (1979).

16) J. Tardy, R. Meandre, *Duilos. Mag. B (UK) Vol.48, No.6*, 571 (1983).

17) J.C. Knigth, R.A. Lujan, M.P. Rossanblum, R.A. Street and D.K. Bieglesen, *Appl. Phys. Lett. 38 (5)*, (1981).

18) N.K. Das, P. Chandhuri and S.T. Kshirager , *J. Appl. Phys. 80 (9)*, (1996).